J. Fluid Mech. (1988), *vol.* 189, *pp.* 243–264
Printed in Great Britain

Effect of vortex shedding on the coupled roll response of bodies in waves

By M. J. DOWNIE,
Department of Naval Architecture and Shipbuilding, The University, Newcastle upon Tyne, NE1 7RU, UK

P. W. BEARMAN AND J. M. R. GRAHAM
Department of Aeronautics, Imperial College, London, SW7 2BY, UK

(Received 9 February 1987 and in revised form 10 September 1987)

Hydrodynamic damping of floating bodies is due mainly to wave radiation and viscous damping. The latter is particularly important in controlling those responses of the body for which the wave damping is small. The roll response of ship hulls near resonance in beam seas is an example of this. The present paper applies a discrete vortex method as a local solution to model vortex shedding from the bilges of a barge hull of rectangular cross-section and hence provides an analytic method for predicting its coupled motions in three degrees of freedom, including the effects of the main component of viscous damping. The method provides a frequency-domain solution satisfying the full linearized boundary conditions on the free surface.

1. Introduction

Calculation of the flows associated with ship motions is usually based on linear potential flow theory, see for example Newman (1977), and with one notable exception, the response of a ship to regular waves is generally well predicted by this theory. Damping is associated with the waves which radiate out from the body due to its motion. But in situations in which the radiated waves are relatively small, that is when the system is lightly damped, the main contribution of the surface waves is to provide a forcing function. This effect is conspicuously evident in the case of roll, particularly near resonance, when the response can be greatly overpredicted by linear theory (Salvesen, Tuck & Faltinsen, 1970), see figure 1. This deficiency in methods based purely on linear potential theory has been overcome, for engineering purposes at least, by incorporating empirical, or semi-empirical, coefficients into the calculation procedures. It has been found that increasing the roll damping coefficient by an appropriate amount leads to good agreement between predicted and experimental results. The underlying rationale and methods for choosing the damping coefficient vary from practitioner to practitioner (Himeno 1981).

The results of a semi-empirical method developed by Tanaka (1961) to predict wave and viscous damping are shown in figure 1. Examples of other approaches are the work of Ikeda, Himeno & Tanaka (1978), who attempted to determine experimentally the individual components of the roll damping (due to the effects of skin friction, flow separation from the hull and its appendages, dynamic lift and wave damping), and of Kaplan, Jiang & Bentson (1982), based on the concept of crossflow drag on the hull and its appendages.

For engineering purposes the motion of floating bodies can be predicted more or

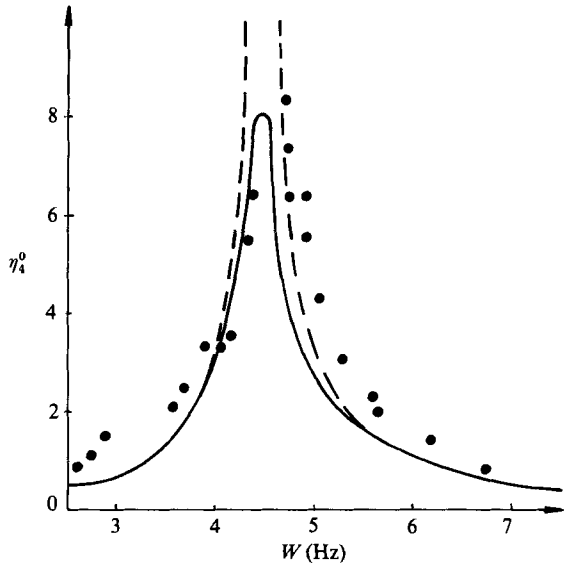

FIGURE 1. Roll amplitude *vs.* frequency for a rectangular cylinder in beam waves (Salvesen *et al.* 1970). ——, wave and viscous damping; – – –, wave damping only; ●, experiment.

less reliably using semi-empirical methods (in the case of conventional hull forms) and empirical methods (for unusual vessels and other marine structures). Such calculations, however, yield little information about the basic physics of the flow, although they do for the most part imply the presence of nonlinearities associated with viscous effects. The physical causes of the discrepancy between responses predicted by linear potential theory and those found in practice have been studied by a number of investigators. One explanation that has been offered is that the differences are simply due to the fact that certain higher-order effects have been neglected. Denise (1982) for example has suggested that they are due to 'water-structure interactions in the splash zone' which could be accounted for by using nonlinear restoring coefficients in the equations of motion. The majority of papers in the literature, on the other hand, make use of equivalent linear viscous roll damping coefficients, implying that there is additional damping due to nonlinearities arising from viscous effects. It is difficult to find incontravertible evidence in support of either point of view and it is probable that either or both phenomena can significantly affect the motions, depending on the ambient conditions. However, models that only incorporate nonlinear restoring forces (Denise 1982; Robinson & Stoddart, 1986) are unable to account completely for the measured response. In order to do so, they also require the inclusion of viscous damping coefficients. In contrast, it has not been found necessary under normal conditions to incorporate nonlinear restoring forces into models that already allow for viscous damping effects.

Of the other factors that may be expected to influence the roll motion of a ship, the effect of surface tension, even at scales of the order commonly used in model testing, has been found to be negligible (Ueno 1949). Similarly the effect of skin friction on the hull has been shown to be small and can be ignored for most practical purposes (Kato 1958). On the other hand, the viscous effects associated with flow separation from the hull and its appendages, particular if they are sharp edged or of small curvature, and also, if the vessel has forward speed, the effect of dynamic lift (Schmitke 1978), can make significant contributions.

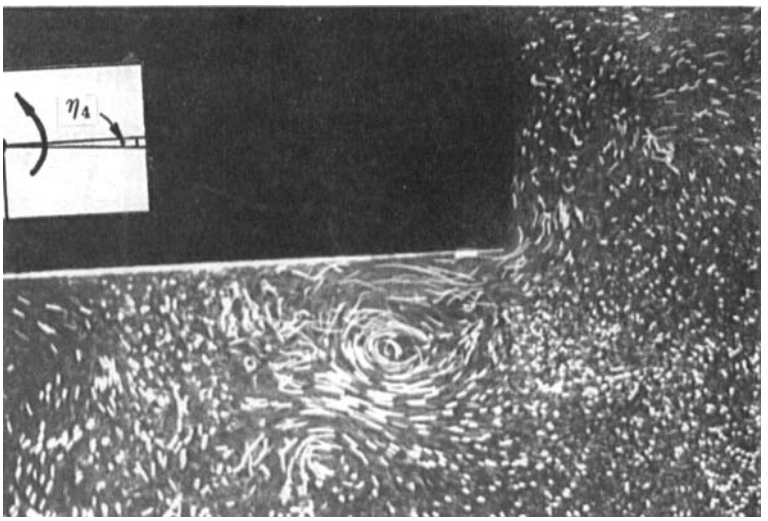

FIGURE 2. Vortex shedding from bilge corner of model barge during forced roll experiments.

Flow-visualization experiments of rolling motion show that separation from the hull surface does occur, particularly if it has sharp edges and appendages. A flow visualization of a forced roll experiment carried out on a model barge in a wave flume is shown in figure 2. During the experiment it was observed that shear layers separating from the bilge corner rolled up to form vortices in a manner very similar to that displayed by oscillatory flows of small displacement amplitude about sharp-edged cylinders. The process will be discussed in more detail at a later stage.

Other experimental evidence suggests the existence of a viscous damping moment proportional to the square of both the frequency and the amplitude of roll (Himeno 1981). Furthermore, it has been observed that the roll amplitude of a sharp-edged barge is smaller than that of a similar vessel with rounded edges in identical conditions, although the roll response was nonlinear in both cases (Brown, Eatock Taylor & Patel 1983). This is consistent with the idea of nonlinear damping due to vortex shedding, the forces due to separation from a rounded bilge being smaller than those due to separation from a sharp one. The subject has been considered in more detail in the discussion of a paper by Robinson & Stoddart (1986) presented at the RINA spring meeting.

Overall, the available evidence suggests that providing the motions are not extreme the most significant factor inducing roll damping is flow separation from the hull surface. The present paper describes a theoretical method for predicting this effect for the case of a flat-bottom, wide-beam, shallow-draught barge of rectangular section floating in regular beam waves at small amplitudes. This problem is well defined in terms of flow separation from the hull surface and is of considerable practical interest since ocean-going barges of this type are used to transport offshore structures. Accurate assessment of roll response must be made before a tow out can take place.

2. Discrete vortex modelling of flow separation at a bilge corner

The flow round a bilge corner is essentially a high-Reynolds-number oscillatory flow in which separation is fixed by the geometry of the body. Vortex formation in

this flow has some similarities to that in impulsively started flows. Flows of this nature having a strong vortex structure are more easily modelled by the discrete vortex method than by a full numerical solution of the Navier–Stokes equation. The discrete vortex method provides a time domain solution for separated flow about bluff bodies. At separation the Kutta–Joukowski condition is satisfied and the bodies themselves are modelled by conformal mapping techniques or by the use of distributions of surface singularities (the boundary integral equation method). Variations of the discrete vortex method relevant to the present work have been reviewed by Graham (1985). Fink & Soh (1974) first used the discrete vortex method to investigate the effect of bilge keels on heave damping, and also considered the development of bilge vortex sheets and the resulting nonlinear forces for slender ships in manoeuvre situations. More recently Ikeda & Himeno (1981) used the method to investigate the influence of viscous effects on the damping of a ship subjected to large-amplitude sway.

In addition to the experimental work described earlier, Brown & Patel (1981) proposed a discrete vortex model for forced barge roll (motion about a fixed roll centre) in which the barge was represented by a semi-infinite body rather than a realistic cross-section. Results of computations based on this geometry and presented in subsequent papers (e.g. Patel & Brown 1986) are difficult to assess, partly because the boundary conditions were not rigourously formulated, and partly because there was no representation of the free surface. The lack of a free surface required a number of assumptions concerning the physics of the flow, and the inclusion of some empirically established factors.

The problem of forced barge roll was also investigated by Bearman, Downie & Graham (1982), who modelled the free surface and barge with a Schwartz–Christoffel transformation and satisfied the boundary conditions on the body using a distribution of source singularities. The results of a parametric study of forced barge roll showed good agreement between the scale of predicted and observed vortices, and between predicted and experimental damping coefficients. They also demonstrated the dependence of the damping coefficient on the location of the roll centre and the barge geometry.

Variations of the discrete vortex method have also been used to calculate the force on ships in still water subjected to a transverse current (Faltinsen, Aarsnes & Pettersen 1965) and to compute two-dimensional eddy-making damping coefficients for incorporation into an analysis of the slow drift oscillations of moored ships (Faltinsen & Sortland 1967). The earlier analysis employed a multi-point vortex tracking method involving the solution for the velocity potential in terms of a distribution of sources and dipoles over the body surface and free shear layers at each timestep. The lengthy computations required by this method were avoided in the later analysis by using the Brown & Michael (1955) approach in which each bilge vortex was represented by a single concentrated vortex. The slow drift oscillation of moored ships is a low-frequency phenomenon and so the problem was further simplified by ignoring the higher-frequency wave motions and formulating it in the low-frequency limit. Faltinsen & Sortland present vortex force coefficients but do not give any results for the motion responses.

Whilst it is probably the most promising way forward at the present time, problems in ship hydromechanics are expensive to compute as time histories by this discrete vortex method and it is often difficult to carry out the computation for a sufficiently long time to attain steady conditions. One way of circumventing this problem is to evaluate the vortex force coefficients from generalized results of a

discrete vortex analysis of flow about an isolated edge. This 'inner' flow is matched to a corresponding 'outer' linearized potential flow about the bilge of a vessel responding to specific wave or other excitation forces. In this way one time-consuming vortex calculation can be used to provide results for a complete range of motions for any given vessel. This method differs from others known to the authors in that it can predict the coupled motion of the barge in three degrees of freedom and is capable of generalization to all six degrees of freedom. It also satisfies the full linearized boundary conditions at the free surface and so is not constrained by a low-frequency limit (i.e. a flat rigid free surface assumed by other vortex computations), and it provides a solution in the frequency domain and so is computationally relatively efficient.

In the case of roll, sway and heave motion in beam seas, a two-dimensional flow field is assumed. The outer flow field associated with the general motion of the barge is solved by a full boundary integral method. Since this method is based on an inviscid potential flow theory which cannot model flow separation, singularities occur at the bilge corners. The inner region is solved using the discrete vortex method applied to flow about a single edge, in which the Kutta–Joukowski condition ensuring smooth separation is satisfied. The matching of the two flows may be viewed as being analogous to the replacement of the outer flow singularities at the bilge corners with physically realistic inner flows in which separation occurs. The method assumes that the flows associated with each edge do not interact and also that the wave-making effects of the vortices are insignificant. The first assumption is justified providing the roll amplitudes are sufficiently small. The results of the method are in fact in reasonable agreement with measured data up to moderately large roll angles. The second assumption is consistent with observations of the behaviour of the model barge in the flow visualization experiment mentioned previously. In addition, in order to incorporate the vortex forces into a conventional motion response computation in the frequency domain it is necessary to ignore the higher harmonics from the nonlinear vortex forces. In practice these harmonics contribute less than 10% to the vortex forces. Their effect is negligible at resonance but could be important at harmonics of the resonant frequency. However, accurate response predictions are not usually so necessary at these higher frequencies.

3. Oscillatory flow about an isolated edge

Oscillatory flow of amplitude $\hat{U}$ and period T about a body of diameter d may be characterized by the Keulegan–Carpenter number, $KC = \hat{U}T/d$. At small KC the maximum displacement of the fluid particles in the undisturbed flow is small in comparison with the scale of the body. Thus vortices may only move away from its edges under the influence of the velocity fields of other vortices shed from those same edges, and hence the shedding from a single edge may become independent from the shedding from other edges. In these circumstances, the local flow becomes analogous to that of oscillatory flow about an infinite wedge. Experiments on sharp-edged bluff bodies (Singh 1979) have shown that at low KC, vortices shed from any given edge at each half cycle form pairs that convect away from the body, and localized shedding occurs.

The discrete vortex analysis of shedding from an isolated edge carried out by Graham (1980) assumed that this type of paired shedding occurs. A typical flow field predicted by this method after four cycles is shown in figure 3. Computations were carried out for a series of infinite wedges of varying internal angle δ.

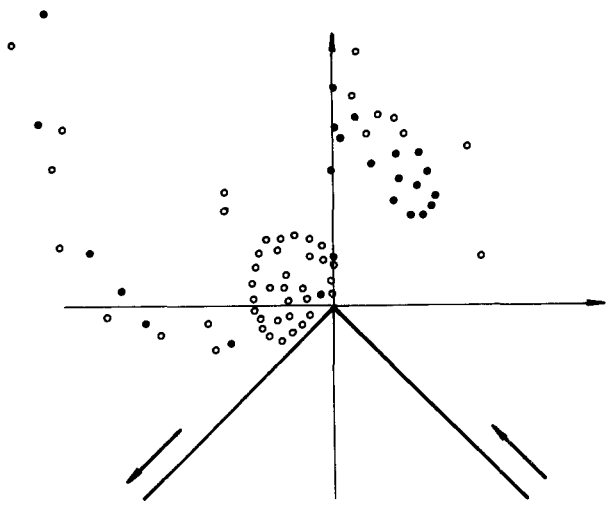

FIGURE 3. Discrete vortex representation of flow about isolated edge (Graham 1980). ●, vortices shed on previous half cycle; ○, vortices shed on current half cycle; →, direction of flow.

The complex force, F_v due to vortex shedding was related to the vortex strengths and positions by

$$F_v = -i\rho \frac{\partial}{\partial t}[\sum_n \Gamma_n(\zeta_n - \zeta_n^*)]. \tag{1}$$

This result can be deduced from Blasius theorem or momentum considerations (Graham 1980).

Γ_n is the strength of the nth discrete vortex located at the point ζ_n in the transformed plane and whose image is located at ζ_n^*. The vortex force may also be written in the form

$$F_v = \tfrac{1}{2}\rho \hat{U}^2 L K C^{(3-2\lambda)/(2\lambda-1)} \Psi, \tag{2}$$

where $\lambda = 2 - \delta/\pi$ and Ψ is a dimensionless function of time. The force was found to act at right angles to the bisector of the infinite wedge.

Since the wedge is infinite, it provides no natural lengthscale. However, there is a lengthscale L implicit in the transformation

$$z = L^{1-\lambda}\zeta^\lambda, \tag{3}$$

mapping a wedge in the z-plane into a half-plane in the ζ-plane. It can be defined as the distance from the edge of a point z_p in the real plane that is equal to the distance from the origin of the corresponding point ζ_p in the transformed plane, i.e. $L = |Z_p|$ for $|Z_p| = |\zeta_p|$.

These wedge flows may be matched to the inner region of an oscillatory flow (amplitude $\hat{U}$ and period T) past a finite body with the same edge angle δ. In that case the lengthscale must be related also to U and T in order that the attached flow velocity U should be the same for both. The complex potential for the attached flow round a wedge is:

$$W = U\zeta, \tag{4}$$

where U is a velocity scale. In terms of this the maximum amplitude of attached flow velocity on the surface of the wedge $q(L_e)$ at a distance L_e from the edge is given by

$$q(L_e) = \frac{1}{\lambda}\hat{U}L^{(\lambda-1)/\lambda}(L_e)^{(1-\lambda)/\lambda}. \tag{5}$$

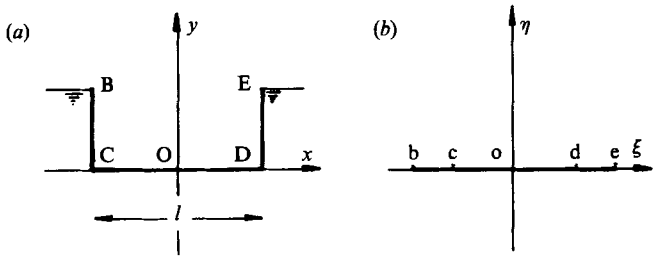

FIGURE 4. Barge transformation. (*a*) Real plane, $z = x+iy$. (*b*) Transformed plane, $\zeta = \xi+i\eta$.

$$z = \int_0^{\zeta} \left(\frac{\zeta^2-\zeta_d^2}{\zeta^2-\zeta_e^2}\right)^{\frac{1}{2}} d\zeta \rightarrow (a_1 l)^{-\frac{1}{2}}\zeta^{\frac{3}{2}}, \quad z = z_D.$$

Therefore, if the timescale of the flow is taken as the period, T, the lengthscale is

$$L_e \propto \hat{U} L^{(\lambda-1)/\lambda}(L_e)^{(1-\lambda)/\lambda}T, \tag{6}$$

i.e.

$$\frac{L_e}{L} \propto \left(\frac{\hat{U}T}{L}\right)^{\lambda/(2\lambda-1)}. \tag{7}$$

The in-line force on a bluff body in sinusoidal flow, $U = \hat{U}\sin\theta$, $(\theta = \omega t)$, is commonly given by Morison's equation

$$\frac{F}{\frac{1}{2}\rho\hat{U}^2 d} = \frac{\pi^2}{KC}C_m \cos\theta + C_D \sin\theta\,|\sin\theta|, \tag{8}$$

where C_m is the inertia coefficient and C_D is the drag coefficient, the drag being entirely due to vortex shedding. The inertia coefficient may be split into two parts, C_{mo} associated with the attached flow, and C_{mv} with the effects of vortex shedding. In the case of bodies which are symmetric with respect to the direction of the flow, the overall force coefficients C_D and C_m may be found straightforwardly from the vortex force in the matched infinite wedge flow. A more detailed account of this procedure is given in Bearman *et al.* (1985). However, this result does not hold for asymmetric bodies, such as the immersed part of the hull of a rolling barge, due to the fact that generally the pressure field associated with vortex shedding at an edge is significant on parts of the body remote from the edge.

4. The vortex forces due to shedding at bilge corners

If a rectangular barge in still water is represented in the complex plane, the z-plane, as shown in figure 4, and sources are distributed over its surface so as to satisfy the boundary conditions arising out of its subsequent motion, the complex force Z and the roll moment about the origin M_0 may be calculated respectively from

$$Z = X + iY = i\int_B p\,dz, \tag{9}$$

$$M_0 = \int_B p\,\mathrm{Re}\{\bar{z}\,dz\}, \tag{10}$$

where,

$$p = -\rho\left(\tfrac{1}{2}q^2 + \frac{\partial\phi}{\partial t}\right) \tag{11}$$

is the pressure, q is the surface velocity, ϕ is the velocity potential, $\bar{z}$ is the complex conjugate of $z = x + iy$ and the integration is carried out over the body surface (B).

In calculating the pressure field and forces on a body in waves using linear potential theory, it is conventional to ignore the q^2 term in the unsteady Bernoulli equation for the pressure, since it is second order in the wave height and motion amplitude. The following analysis similarly ignores the q^2 term associated both with the attached flow and also with vortex shedding and so cannot be regarded as complete to second order. However, in addition to the usual $\partial\phi/\partial t$ term associated with the attached flow, the $\partial\phi/\partial t$ term associated with vortex shedding will be included. The aim of the present analysis is to evaluate the lowest-order contribution to the pressure due to vortex shedding, on the basis that this is the dominant term for conditions such as roll motion for which the first-order radiation damping becomes very small. The q^2 term associated with vortex shedding is therefore ignored because its contribution is the same size as the wave potential contribution to $|\nabla\phi|^2$, since the Kutta–Joukowski condition shows that the two must be equal and opposite at the separated side of the edge. In addition, because of its image effect the vortex contribution towards the velocity field will be seen to be like that of a dipole at large distances r from the edge, falling off as r^{-2}. The effect of this component on overall forces and moments on the body is therefore limited to a small region in the vicinity of the edge of size proportional to the lengthscale of the vortices.

The $\partial\phi/\partial t$ term associated with the vortex shedding, although also of second order, is retained because its contribution to the pressure falls off as r^{-1} and so makes a significant contribution to the force and moments from the whole of the body surface. This is consistent both with the fact that linear potential theory alone cannot adequately predict roll responses and also that the experimental evidence, as discussed previously, indicates that vortex shedding makes the major contribution to the roll damping when the linear wave damping is comparatively small. The observations of Brown *et al.* (1983) concerning the reduction of roll damping obtained by rounding sharp-edged bilges are particularly significant in this respect.

The contribution made to the complex potential by N discrete vortices shed from a bilge edge, W_v, may be written as

$$W_v = \sum_{n=1}^{N} \frac{i\Gamma_n}{2\pi} [\log(\zeta - \zeta_n) - \log(\zeta - \zeta_n^*)], \tag{12}$$

where ζ_n is the location of the nth vortex of strength Γ_n, ζ_n^* is the location of its image and W_v is always real when ζ lies on the surface of the barge. The corresponding pressure field is

$$P_v = -\rho\frac{\partial\phi}{\partial t} = \rho \sum_{n=1}^{N-1} \frac{i\Gamma_n}{2\pi}\left[\frac{\zeta_n}{\zeta - \zeta_n} - \frac{\zeta_N^*}{\zeta - \zeta_n^*}\right] - \rho\frac{i\Gamma_N}{2\pi}\log\left(\frac{\zeta - \zeta_N}{\zeta - \zeta_N^*}\right), \tag{13}$$

where the Nth discrete vortex is the last to be shed and is the only one whose strength is changing with time. The first term in the pressure equation is continuous and has a finite value of

$$-\rho \sum_{n-1}^{N-1} \frac{\Gamma_n}{\pi}\frac{d}{dt}(\mathrm{Arg}[\zeta_d - \zeta_n]).$$

The second term is finite but discontinuous, having a jump of $\rho(\partial\Gamma_N/\partial t)$ at the edge.

Introducing the location of the shedding edge ζ_d into the complex potential, and expanding leads to

$$W_v = -\sum_{n=1}^{N} \frac{i\Gamma_n}{2\pi} \frac{\zeta_n - \zeta_n^*}{\zeta - \zeta_d} + O\left(\frac{\zeta_n - \zeta_n^*}{\zeta - \zeta_d}\right)^2. \tag{14}$$

The pressure on the surface of the barge can therefore be represented by the dipole-like expression

$$P_v = \rho \frac{\partial}{\partial t} \sum_{n=1}^{N} \frac{i\Gamma_n}{2\pi} \frac{\zeta_n - \zeta_n^*}{\zeta - \zeta_d}, \tag{15}$$

which holds everywhere except very close to the bilge edge ζ_d. The difference between the full equation and the dipole approximation for the vortex induced pressure P_v over the surface of the barge is only significant over a region of order $|\zeta_n - \zeta_d|$ around the bilge edge. Therefore the lowest-order term, with respect to the amplitude of motion, of the pressure distribution on the body due to vortex shedding is given by the dipole approximation.

In order to calculate the complex force and the moment on the body, it is convenient to integrate the pressure in the transformed plane. In the case of a rectangular barge, as shown in figure 4, the two planes are related by the Schwartz–Christoffel transformation

$$z = \int_0^{\zeta} \left(\frac{\zeta^2 - \zeta_d^2}{\zeta^2 - \zeta_e^2}\right)^{\frac{1}{2}} d\zeta, \tag{16}$$

where ζ_d and ζ_e in the transformed plane correspond to the bilge edges z_D and z_E in the physical plane, and it is a necessary property of the transformation that

$$\frac{dz}{d\zeta} \to 1, \quad z, \zeta \to \infty. \tag{17}$$

In the vicinity of a shedding edge, z_D for example, it may be seen that

$$|z'| = |z - z_D| \to \frac{2}{3}\left(\frac{2\zeta_d}{\zeta_e^2 - \zeta_d^2}\right)^{\frac{1}{2}} \zeta'^{\frac{3}{2}} \quad z, \zeta \to z_D, \zeta_d, \tag{18}$$

where $\zeta' = \zeta - \zeta_d$. This latter property of the transformation is used in matching the local flow about a shedding edge to an exterior flow associated with the barge responding to excitation by regular waves.

The complex force Z_v on the barge due to vortex shedding from a single edge is therefore given by

$$\begin{aligned} Z_v &= i\rho \int_B \frac{\partial}{\partial t}\left[\sum_{n=1}^{N} \frac{i\Gamma_n}{2\pi} \frac{\zeta - \zeta_n^*}{\zeta - \zeta_d}\right] dz \\ &= i\rho \frac{\partial}{\partial t}\left[\sum_{n=1}^{N} \Gamma_n(\zeta - \zeta_n^*)\right] a_{fv}. \end{aligned} \tag{19}$$

Similarly, the moment M_0 about the origin due to vortex shedding from one edge is given by

$$\begin{aligned} M_0 &= \rho \int_B \frac{\partial}{\partial t}\left[\sum_{n=1}^{N} \frac{i\Gamma_n}{2\pi} \frac{\zeta - \zeta_n^*}{\zeta - \zeta_d} \operatorname{Re}\{\bar{z}\, dz\}\right] \\ &= -i\rho \frac{\partial}{\partial t}\left[\sum_{n=1}^{N} \Gamma_n(\zeta_n - \zeta_n^*]\right] a_{mv}. \end{aligned} \tag{20}$$

The term

$$\frac{\partial}{\partial t}\left[\sum_{n=1}^{N} \Gamma_n(\zeta_n - \zeta_n^*)\right],$$

is a universal vortex shedding factor which can be obtained from a discrete vortex computation of vortex shedding from an isolated right angled edge in oscillatory flow, see equation (1). The coefficients a_{fv} and a_{mv} are given respectively by the integral expressions

$$a_{\mathrm{fv}} = -\frac{\mathrm{i}}{2\pi}\int_B f(\zeta)\,\mathrm{d}\zeta = -\frac{\mathrm{i}}{2\pi}\int_B \frac{(\zeta^2-\zeta_{\mathrm{d}}^2)^{\frac{1}{2}}}{(\zeta-\zeta_{\mathrm{d}})(\zeta^2-\zeta_{\mathrm{e}}^2)^{\frac{1}{2}}}\,\mathrm{d}\zeta, \tag{21}$$

$$a_{\mathrm{mv}} = I_m\left\{\frac{\mathrm{i}}{2\pi}\overline{\left[\int_0^{\zeta}\left(\frac{\zeta^2-\zeta_{\mathrm{d}}^2}{\zeta^2-\zeta_{\mathrm{e}}^2}\right)^{\frac{1}{2}}\mathrm{d}\zeta\right]}f(\zeta)\,\mathrm{d}\zeta\right\}, \tag{22}$$

where the overbar signifies the complex conjugate. The integrals depend only on the barge geometry and can be calculated straightforwardly in the transformed plane. Consequently the computationally expensive vortex calculation may be separated from the particular geometry of the barge and its motion, and need in principle be done only once to provide the factor for all cases having the same bilge edge angle.

5. Matching the edge flows

The total flow field about a barge responding to waves may now be found by matching locally the flow in an outer region, calculated by the boundary integral method described previously or some other potential flow method, to the flow in an inner region given by the discrete vortex analysis of oscillatory flow about an infinite wedge. The matching is carried out in the transformed plane where both velocity fields are finite at the edge so as to avoid the singularity which would occur at that point in the real plane (see figure 5).

The transformation that maps an infinite wedge into a half-plane is

$$z = \mathrm{e}^{-\mathrm{i}\frac{1}{2}\pi} L^{-\frac{1}{2}} \zeta^{\frac{3}{2}}, \tag{23}$$

where L is the lengthscale implied by the transformation as discussed previously. The transformation that maps a barge of rectangular section into a half-plane, in the near vicinity of the shedding edge (see (18)) is

$$\begin{aligned} z &= \mathrm{e}^{-\mathrm{i}\frac{1}{2}\pi}\frac{2}{3}\left(\frac{2\zeta_{\mathrm{d}}}{\zeta_{\mathrm{e}}^2-\zeta_{\mathrm{d}}^2}\right)^{\frac{1}{2}}\zeta^{\frac{3}{2}} \\ &= \mathrm{e}^{-\mathrm{i}\frac{1}{2}\pi}(a_l\, l)^{-\frac{1}{2}}\zeta^{\frac{3}{2}}. \end{aligned} \tag{24}$$

The geometry of the barge is identical with that of the wedge close to their respective edges provides that

$$L = a_l\, l, \tag{25}$$

which makes the transformations identical.

The velocity in the physical plane, U_z, is related to the velocity in the transformed plane, u_ζ, by

$$U_z = u_\zeta \frac{\mathrm{d}\zeta}{\mathrm{d}z}. \tag{26}$$

If the lengthscales are matched (equation (25)) and the transformed edge velocity for the barge, u_{B}, is the same as the transformed edge velocity for the wedge, u_{e}, then

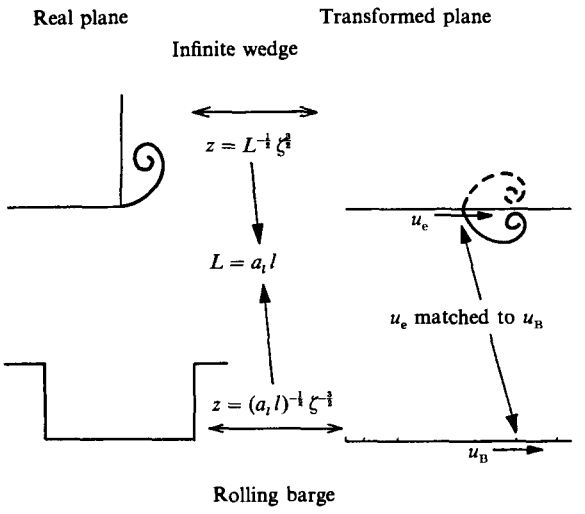

FIGURE 5. Matching the local and exterior flows.

the flows around the edges in the physical planes are also identical. It may be seen from equations (1), (2) and (19), therefore, that the complex force on a barge due to vortex shedding from one of its bilge corners is

$$Z_v = \tfrac{1}{2}\rho\hat{U}^2 L K C^{(3-2\lambda)/2\lambda-1}\,\Psi a_{fv}, \tag{27}$$

if $\hat{U} = \hat{u}_e = \hat{u}_B L = a_l l$. The moment about the point O is

$$M_0 = \tfrac{1}{2}\rho\hat{U}^2 L K C^{(3-2\lambda)/2\lambda-1}\,\Psi a_{mv}. \tag{28}$$

The vortex forces experienced by a floating barge, then, can be found from the discrete vortex analysis of an infinite wedge, matched to each bilge, and the calculation of the flow velocity u_B given by potential (attached flow) theory in the transformed plane at points corresponding to the edges of the bilges. The calculation of u_B generally involves a fairly lengthy computation.

6. Calculation of the exterior flow field

The exterior wave flow field is described by a velocity potential which satisfies Laplace's equation. This potential Φ may be written in terms of the components for each wave frequency ω:

$$\Phi(x,y,z,t) = \phi_0 e^{-i\omega t} + \sum_{j=1}^{6} \phi_j \dot{H}_j + \phi_7 e^{-i\omega t}, \tag{29}$$

where ϕ_0 is the potential for the undisturbed incident wave, ϕ_7 for the wave scattered by the ship considered as a fixed body, and ϕ_j for the waves radiated by the ship when moving in its six rigid body modes, $H_j = \eta_j e^{i\omega t}$, (1 surge, 2 sway, 3 heave, 4 roll, 5 pitch and 6 yaw). Where it is understood that the real part only of the potential is considered. Z is the longitudinal axis of the hull parallel to the roll axis. Each component of the potential satisfies the linearized free surface condition

$$-\omega^2\phi_j + g\frac{\partial\phi_j}{\partial y} = 0 \quad (j = 0,7, y = 0), \tag{30}$$

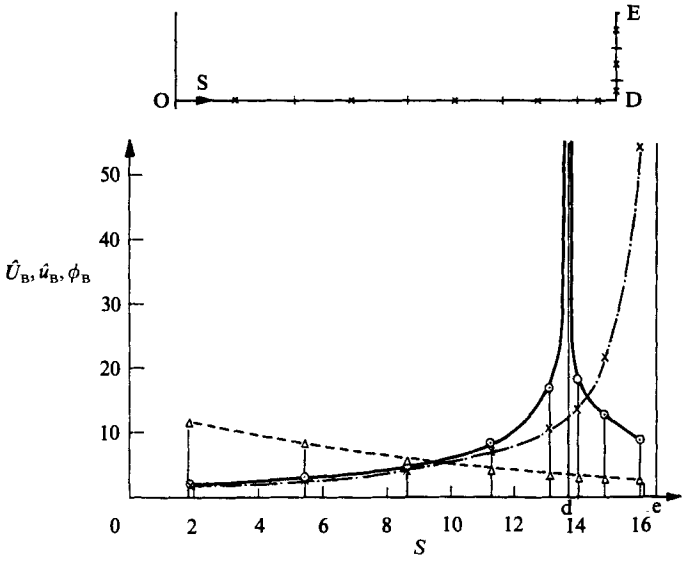

FIGURE 6. Velocity distribution on barge surface. ⊙, velocity amplitude, $\hat{U}_B$, in real plane; ×, velocity amplitude, $\hat{u}_B$, in transformed plane; △, phase angle, ϕ_B.

and, except for ϕ_0 a normal velocity condition on the body and the sea bed and a radiation condition.

In this paper we use the source panel method to represent the potentials. Thus

$$\phi_j(q') = \frac{1}{4\pi}\int_B \sigma_j(q)\, G(q', q)\, \mathrm{d}s \quad (j = 1, 7). \tag{31}$$

The integral is over the points q lying on the wetted surface of the ship in its still water position, $\sigma(q)$ are the source densities and $G(q', q)$ are suitable Green functions (John 1950). The potentials are evaluated by solving the boundary integral equations on the surface of the ship numerically (e.g. Brown *et al.* 1983).

The equations of motion of the freely floating body can conveniently be expressed as

$$\sum_k [-\omega^2(M_{jk}+A_{jk}) - \mathrm{i}\omega B_{jk} + C_{jk}]\,\eta_k = f_j, \tag{32}$$

where $\boldsymbol{M}$ is the mass matrix, $\boldsymbol{A}$ is the added-mass matrix, $\boldsymbol{B}$ is the matrix of damping coefficients, $\boldsymbol{C}$ is the matrix of restoring coefficients and f_j are the complex amplitudes of the exciting forces and moments. The added-mass, damping and exciting forces are calculated from the linearized form of Bernoulli's equation:

$$p = -\rho\left(\frac{\partial\phi}{\partial t}\right) + gy, \tag{33}$$

using the values of the potentials given by the boundary integral method.

In the present case the problem is considerably simplified by following Salvesen *et al.* (1970) and using strip theory – that is, by reducing the three-dimensional solution to a series of two-dimensional solutions carried out at a number of transverse sections along the hull and integrating over its length, L_z. Under these conditions the three-dimensional Laplace equation and the boundary conditions for the potential

reduce to those appropriate to the two-dimensional problem of a body with cross-section C_z oscillating in the free surface.

The potentials may be found using a standard two-dimensional panel method using panels of constant source density and line singularity approximations for the far-field effect of each panel. The method has been tested on a ship section for which Vugts (1971) has presented results and good agreement was obtained.

By solving the equations of motion and taking the appropriate derivative of the potential, the relative velocity on the surface of the vessel may be determined at points adjacent to and on either side of the bilge edges. The matching of the interior and the exterior flows is carried out in the transformed plane because the attached flow velocity field is singular at the edges in the real plane but finite at the corresponding points in the transformed plane. The velocity amplitude, U_{Bj}, at a point ζ_j in the transformed plane is given by the relationship

$$\hat{u}_{Bj} = \hat{U}_{Bj}\left(\frac{dz}{d\zeta}\right)_j. \tag{34}$$

The velocity amplitude at the point in the transformed plane corresponding to the bilge edge is obtained by interpolation. An example of the velocity distribution over the barge surface in both planes is shown in figure 6.

7. Inclusion of vortex forces in the barge response calculations

In the interests of simplicity, the expressions for the vortex induced force and moment will be derived for shedding for one edge only. The overall force may be obtained by summing the forces at each edge.

The barge motions (see equation (2)) may be written as

$$H_j = \hat{\eta}_j \cos(\theta - \epsilon_j) = \hat{\eta} \cos\theta_j, \tag{35}$$

where $\hat{\eta}_j$ is the modulus of the complex amplitude η_j and ϵ_j is its argument, that is, the phase angle. Similarly the fluid displacement relative to the edge in the transformed barge plane (see figure 5) is $H_b = \hat{\eta}_b \cos\theta_b$ and in the transformed wedge plane is

$$H_e = \hat{\eta}_e \cos\theta_e = \frac{\hat{U}}{\omega} \cos\theta_e, \tag{36}$$

where $\hat{U}$ is the velocity amplitude of the oscillatory flow about the isolated edge and ω is its frequency.

For a right-angled edge, the vortex force on the isolated edge (see equation (2)) is given by

$$F_{ve} = \tfrac{1}{2}\rho \hat{U}^2 L \Psi, \tag{37}$$

so that the force experienced by the barge becomes

$$F_{vb} = \tfrac{1}{2}\rho\omega^2 \hat{\eta}_b a_l l \Psi a_{fv} \tag{38}$$

providing the flows are matched and $\hat{U} = \omega\hat{\eta}_b$, $L = a_l l$ and $\theta_e = \theta_b$. The dimensionless vortex force function Ψ can be expressed in the form of a Morison equation whose coefficients have been evaluated by Graham (1980), and so the vortex force and moment can be written respectively as

$$F_{vb} = -\tfrac{1}{2}\rho\omega^2\hat{\eta}_b^2 a_l l(\bar{A} \sin\theta_b |\sin\theta_b| + \pi^2 \bar{B} \cos\theta_B) a_{fv}, \tag{39}$$

$$M_{vb} = F_{vb} l a_{mv}. \tag{40}$$

Because of the nonlinear nature of the vortex forces, they give rise to higher harmonics, which computations show to be of the order of 10% of the terms of the fundamental frequency. In order to carry out a response analysis in the frequency plane it is convenient to ignore these higher harmonics of the vortex force. They contribute little at resonance, giving a very small response at harmonics of the input. They may contribute significantly at subharmonics of the resonant frequency for which some resonant response may be excited. However, vessel-response calculations are much less important for these off-resonant frequencies, where the wave damping becomes dominant, so the harmonics may safely be ignored. Thus, the vortex sway and heave forces, $F_{v2} = \mathrm{Re}\{F_{vb}\}$ and $F_{v3} = \mathrm{Im}\{F_{vb}\}$ and the vortex moment $F_{v4} = M_{vb}$ can be expressed in terms of a Fourier series and, ignoring the higher harmonics written as

$$F_{vj} = a_{1j}\cos\theta + b_{1j}\sin\theta = \mathrm{Re}\{f_{vj}\,e^{-i\omega t}\}, \tag{41}$$

where

$$a_{1j} = \frac{1}{\pi}\int_0^{2\pi} f_{vf}\cos\theta\,d\theta, \tag{42}$$

$$b_{1j} = \frac{1}{\pi}\int_0^{2\pi} f_{vj}\sin\theta\,d\theta. \tag{43}$$

The equations of motion with vortex forces included are given by

$$M\ddot{H} = X + F_v,$$

or

$$[-\omega^2(M_{jk}+A_{jk}) - i\omega B_{jk} + C_{jk}]\,\eta_k = f_{vj} + f_j. \tag{44}$$

All the terms in the equations for the vortex force and moment are known with the exception of $\hat{\eta}_b$ and θ_b, because the vortex forces are nonlinear functions of the amplitudes of motion η_j. Solution of the equations therefore requires the use of an iterative procedure. In the present instance, the amplitudes of the motion were determined by minimizing the residuals R_j where,

$$R_j = [-\omega^2(M_{jk}+A_{jk}) - i\omega B_{jk} + C_{jk}]\,\eta_k - f_{vj}(\eta_k) - f_j. \tag{45}$$

8. Results

A preliminary test of the method was the calculation of the damping experienced by a barge undergoing forced roll. The case study chosen was that of a barge whose beam to draught ratio was 10 and whose length was about 3.25 times its beam. The damping, expressed as a percentage of the critical damping, ζ_c, is shown as a function of the roll amplitude in figure 7 and compared with experimental forced roll results carried out on a model. These experimental results are taken from tests carried out by BMT Ltd. As they are proprietary data the comparison is shown here, with their permission, without numerical scales.

The motions of the same barge floating freely in regular beam waves were then computed for a range of frequencies. The roll response for unit wave amplitude, $h_w = 1$, is shown in figure 8, which also shows the results that would have been given by the strip-theory calculation had the vortex forces not been included. Figures 9, 10 and 11 show a comparison of the sway, heave and roll responses with experimental results obtained with $h_w = 0.55\,h_b$, where h_b is the draught of the barge. The experimental results were obtained for a barge of the same dimensions but with slightly rounded bilge corners.

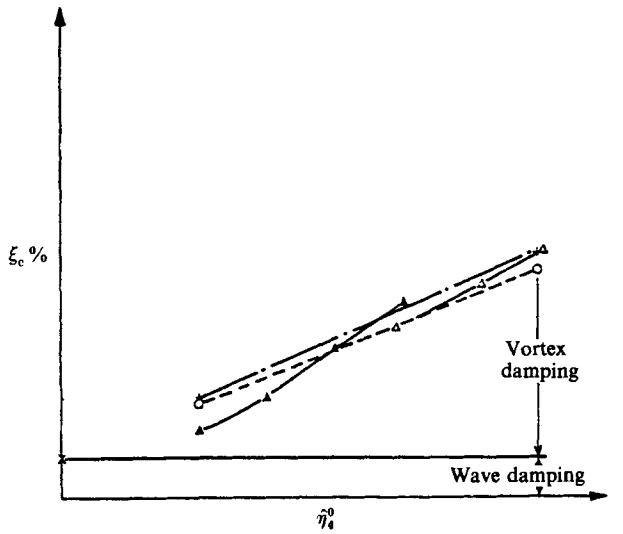

FIGURE 7. Roll damping (expressed as percentage of critical damping, ξ_c) *vs.* roll amplitude for barge undergoing roll at natural frequency. ▲, natural decay tests; △, forced roll tests; ⊙, low-frequency analysis (Bearman *et al.* 1982); +, present theory.

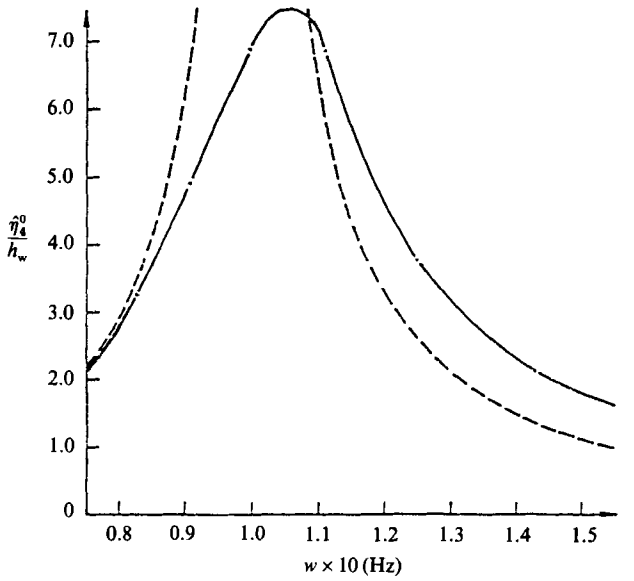

FIGURE 8. Roll response amplitude operator (RAO) *vs.* wave frequency, $h_w = 1$. ———, potential flow calculation; –·–, present theory.

Finally, predictions and measurement of the roll response at the natural roll frequency are shown as a function of the wave amplitude in figure 12.

The damping force predicted by the theory is made up of two components, one of which is proportional to the amplitude of the radiated waves, and the other of which is due to vortex shedding and is proportional to the square of both the frequency and amplitude of the motion for a rectangular body. For forced roll at a given frequency,

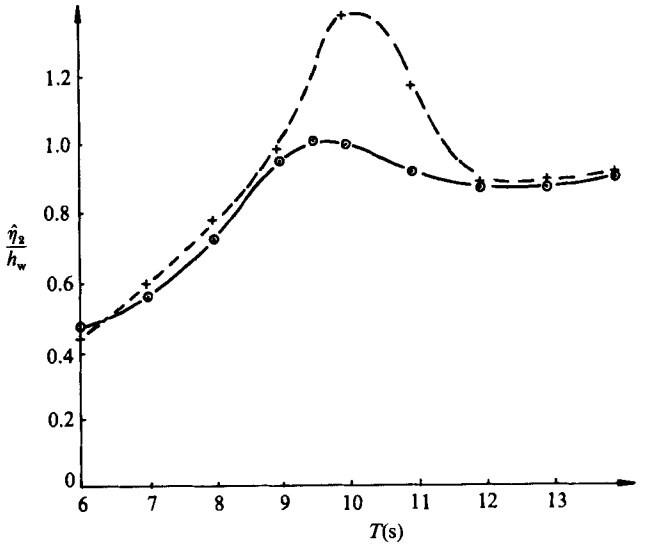

FIGURE 9. Sway RAO *vs.* wave period, $h_w = 0.55\,h_b$. +, round edged barge experimental results; ⊙, sharp edged barge, present theory.

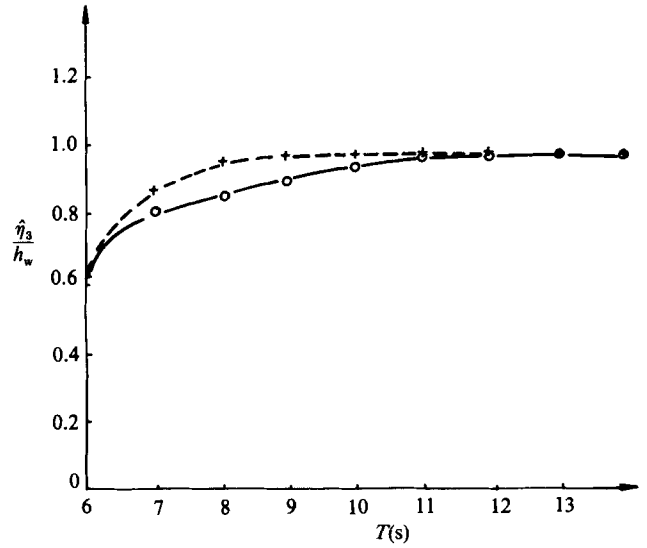

FIGURE 10. Heave RAO *vs.* wave period, $h_w = 0.55\,h_b$. +, round-edged barge experimental results; ⊙, sharp-edged barge, present theory.

this leads to a constant wave-damping coefficient and a vortex-damping coefficient that is linear with the roll amplitude, as shown in figure 7. The calculated and experimental results can be seen to be in good agreement with one another.

The vortex forces are critically dependent upon the relative velocity of the fluid in the immediate vicinity of the bilge corners, which the calculations show to be very sensitive to the location of the roll centre and the barge geometry. Indeed, for any given barge there exists a roll centre for which there is no vortex shedding at all, the bilge corner behaving as a leading edge in a symmetric flow. This dependence of the

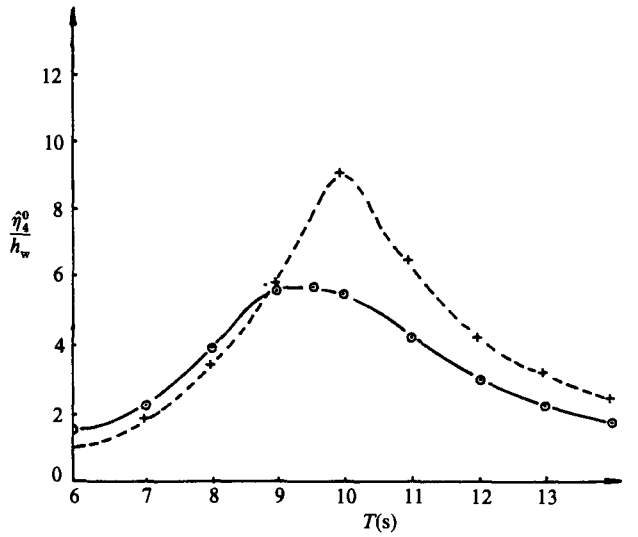

FIGURE 11. Roll RAO *vs.* wave period, $h_w = 0.55\,h_b$. +, round-edged barge experimental results; ⊙, sharp-edged barge, present theory.

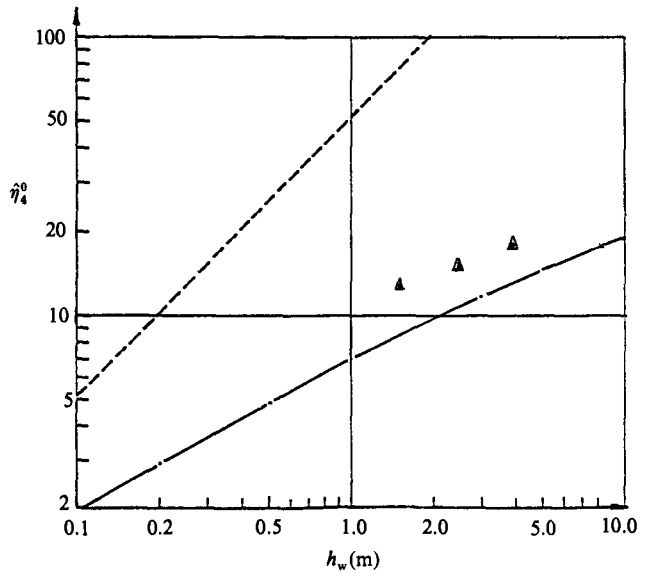

FIGURE 12. Roll amplitude *vs.* wave amplitude at natural roll frequency. △, round-edged barge experimental results; ---, potential flow calculation; –·–, present theory.

vortex damping on the location of the roll centre calls for a closer scrutiny of the practice of using forced roll results for the prediction of the motion of freely floating bodies.

The roll RAO (response amplitude operator, $\hat{\eta}_4/h_w$) of the barge floating freely in regular beam waves is shown in figure 8 and can be seen to be very similar to the results presented by Salvesen *et al.* and shown in figure 1. Both figures show that potential theory alone considerably overpredicts the roll response in the region of

resonance. The theoretical results of figure 8 also show a shift in the resonant frequency similar to that displayed by the experimental results of figure 1.

A comparison of theoretical and experimental results is shown in figures 9, 10 and 11. As might be expected the two are in good agreement away from resonance where vortex shedding has little effect. The discrepancies around resonance, which are small in comparison with those displayed in figure 1, can be explained by the fact that the model used in the experiment had slightly rounded bilges. The vortex forces are smaller for a round edged but otherwise comparable body with sharp edges, and so the damping is also smaller.

The final figure of roll amplitude against wave amplitude demonstrates the nonlinear nature of the response near resonance. Again the results are compared with experimental results for a round-edged barge. The increase in accuracy obtained by including the vortex forces in the calculation is again clearly demonstrated.

9. Conclusions

It has been shown that the motions of a sharp-edged rectangular body floating freely in regular beam waves can be reasonably well predicted in all three degrees of freedom using a purely theoretical method. The result implies that the non-linearities in the responses are largely due to vortex shedding from the body surface providing the motions are not extreme.

We gratefully acknowledge the financial support of BMT Ltd and the SERC Marine Technology Directorate for this work.

REFERENCES

BEARMAN, P. W., DOWNIE, M. J. & GRAHAM, J. M. R. 1982 Calculation method for separated flows with applications to oscillatory flow past cylinders and the roll damping of barges. *Proc. 14th Symp. Naval Hydrodynamics, Ann Arbor, Michigan, USA.*

BEARMAN, P. W., DOWNIE, M. J., GRAHAM, J. M. R. & OBASAJU, E. D. 1985 Forces on cylinders in viscous oscillatory flow at low Keulegan–Carpenter numbers. *J. Fluid Mech.* **154**, 337.

BEARMAN, P. W., GRAHAM, J. M. R., NAYLOR, P. & OBASAJU, E. D. 1981 The role of vortices in oscillatory flow about bluff cylinders. *Intl Symp. Hyd. in Ocean Engng.* Norwegian Inst. Tech.

BROWN, C. E. & MICHAEL, W. H. 1955 The effect of leading edge separation on the lift of a delta wing. *J. Aero. Sci.* **21**, 690.

BROWN, D. T., EATOCK TAYLOR, R. & PATEL, M. H. 1983 Barge motions in random seas – a comparison of theory and experiment. *J. Fluid Mech.* **129**, 385.

BROWN, D. T. & PATEL, M. H. 1981 The calculation of vorticity effects on the motion response of a flat bottomed barge to waves. *Proc. Intl Symp. Hyd. in Ocean Engng.* Norwegian Inst. Tech.

DENISE, J.-P. F. 1982 On the roll motion of barges. *RINA Paper* W10.

FALTINSEN, O., AARSNES, J. V. & PETTERSEN, B. 1985 Application of vortex tracking method to current forces on ships. *Proc. Symp. on Separated Flows about Marine Structures*, Trondheim, Norway.

FALTINSEN, O. & SORTLAND, B. 1987 Slow drift eddy making damping of a ship. *Appl. Ocean Res.* **9**, 37.

FINK, P. T. & SOH, W. K. 1974 Calculation of vortex sheets in unsteady flow and application in ship hydrodynamics. *Proc 10th Symp. Naval Hydrodynamics*, Cambridge, Massachussetts.

GRAHAM, J. M. R. 1980 The forces on sharp-edged cylinders in oscillatory flow at low Keulegan–Carpenter numbers. *J. Fluid Mech.* **97**, 331.

GRAHAM, J. M. R. 1985 Numerical simulation of steady and unsteady flow about sharp edged bodies. *Proc. Symp. on Separated Flows about Marine Structures*, Trondheim, Norway.

HIMENO, Y. 1981 Prediction of ship roll damping – state of the art. *Dept Nav. Arch. and Mar. Engng, Univ. of Michigan, Rep.* 239.

IKEDA, Y. & HIMENO, Y. 1981 Calculation of vortex shedding flow around oscillating circular and Lewis form cylinders. *3rd Intl Conf. Num. Ship Hyd.* Paris.

IKEDA, Y., HIMENO, Y. & TANAKA, N. 1978 A prediction method for ship roll damping. *Dept. Nav. Arch. Univ. of Osaka Prefecture, Rep.* 00405.

JOHN, F. 1980 On the motion of floating bodies, part II. *Commun. Pure Appl. Maths* **3**, 45.

KAPLAN, P., JIANG, C.-W. & BENTSON, J. 1982 Hydrodynamic analysis of barge platform systems in waves. *RINA Spring Meeting, Paper no.* 8.

KATO, H. 1958 On the frictional resistance to the rolling of ships. *J. Soc. Nav. Arch. Japan* **102**, 115.

NEWMAN, J. N. 1977 *Marine Hydrodynamics*. MIT Press.

PATEL, M. H. & BROWN, D. T. 1986 On predictions of resonant roll motions for flat-bottomed barges. *RINA Supplementary Papers*, vol. 128.

ROBINSON, R. W. & STODDART, A. W. 1986 An engineering assessment of the role of non-linearities in transportation barge roll response. *RINA Spring Meeting, Paper no.* 8.

SALVESEN, N., TUCK, E. O. & FALTINSEN, O. 1970 Ship motions and sea loads. *Trans. SNAME* **78**, 421.

SCHMITKE, R. T. 1978 Ship sway, roll and yaw motions in oblique seas. *Trans. SNAME* **86**, 26.

SINGH, S. 1979 Forces on bodies in oscillatory flow. Ph.D. thesis, University of London.

TANAKA, N. 1961 A study on bilge keels. (Part 4. On the eddy making resistance to the rolling of a ship's hull). *J. Soc. Nav. Arch. Japan* **109**, 205.

UENO, K. 1949 Influence of the surface tension of the surrounding water upon the free rolling of model ships. *Report of Res. Inst. for Appl. Mech.* Kyushu University.

VUGTS, J. H. 1971 The hydrodynamic forces and ship motions in oblique waves. *Neth. Ship Res. Centre TNO. Rep.* 150S.